Journal of Materials Science: Materials in Electronics
https://doi.org/10.1007/s10854-018-9957-4

A new glass–ceramic with low permittivity for LTCC application

Denghui Jiang[1] · Jingjing Chen[1] · Baobiao Lu[1] · Juan Xi[1] · Guohua Chen[1]

Received: 25 July 2018 / Accepted: 28 August 2018

Abstract
The phase evolution and dielectric properties of $10CaO–40ZnO–15B_2O_3–35P_2O_5$ (in wt%) glass–ceramics were investigated. Three kinds of crystalline phases including $Ca_2B_2O_5$, $CaZn_2(PO_4)_2$ and $Zn_3(PO_4)_2$ are formed in the sintered glass–ceramics. The dielectric properties change significantly with sintering temperature and phase composition. The optimum microwave dielectric properties of $\varepsilon_r = 4.32$, $Q \times f = 16820$ GHz (at 13.44 GHz) and $\tau_f = -27$ ppm/°C have been achieved after sintering at 740 °C for 2 h. Moreover, the glass–ceramic is chemically compatible with silver (Ag) electrode under the co-fired process. This finding would make the as-prepared glass–ceramic promising candidate for LTCC application.

1 Introduction

Low temperature co-fired ceramic (LTCC) is the important composite of modern microelectronic packaging [1, 2]. Due to the limited sintering temperature capability of metal electrodes such as Ag or Cu, LTCC with sintering temperature below 900 °C have been in great demand. With the development of further miniaturization of electronic devices, it is vital to develop the LTCC substrate materials with low permittivity and dielectric loss to fill the need of high signal propagation speed and high reliability [3, 4]. Advanced substrate materials for microwave integrated circuits require a low dielectric constant ($\varepsilon_r < 5$) to maximize the signal propagation speed, a high quality factor ($Q \times f \geq 5000$ GHz) to increase the frequency selectivity, and a near-zero temperature coefficient of resonance frequency (τ_f) to ensure the stability of the frequency against temperature variations [5].

Commercially available two LTCC dielectrics are glass + ceramics and ceramic materials with original low sintering temperature [6, 7]. However, due to the resonant loss of the glass in high frequency, the former is not suitable for applications in higher frequency. As for the latter, it is very difficult to satisfy the requirement of high signal propagation speed because of the relatively high dielectric constant.

Recently, the applications of glass–ceramic (crystallizable glass) dielectrics with low sintering temperature in LTCC have attracted considerable interest [8]. In fabrication of desirable LTCC glass–ceramics, the crystalline phases are formed during firing. Complete densification and sufficient crystallization are prerequisites for good mechanical properties and high Q-values of the substrate materials. Due to the higher Q-values, the glass–ceramic system seems to be more promising for applications in LTCC modules than glass + ceramics and ceramic materials with original low firing temperature.

Recently, there are several LTCC glass–ceramic systems. Urban Dośler reported that $MgO–B_2O_3–SiO_2$ based (MBS) glass–ceramics sintered at 850–950 °C exhibited the dielectric constants of 6.1–6.9 and $Q \times f$ values of 5000–8000 GHz (at ~ 12 GHz) [9]. Chiang et al. reported that $CaO–B_2O_3–SiO_2$ system glass–ceramics sintered at 850–950 °C showed the dielectric constants of 4.0–7.9 and $Q \times f$ values of ~ 2200 GHz (at ~ 10 GHz) [10]. Compared to the widely-used silicate glasses in the traditional LTCC materials, borate and phosphate glasses have a relatively low soften temperature and crystallization temperature. Induja et al. [11] reported that the $45SnF_2–25SnO–30P_2O_5$ glass possessed the dielectric constant of 16, $Q \times f$ values of 990 GHz (at 6.2 GHz) and temperature coefficient of resonant frequency (τ_f) of − 290 ppm/°C. Yu et al. [8] found that $3ZnO–2B_2O_3$ glass–ceramic sintered at 650 °C displayed a dielectric constant $\varepsilon_r = 7.5$ and $\tan\delta = 6 \times 10^4$ at 10 MHz. For all we know, except for silicate or borate glass–ceramics, no borophosphate glass–ceramic LTCC materials have been reported so far.

✉ Guohua Chen
cgh1682002@163.com

[1] School of Material Science and Engineering, Guilin University of Electronic Technology, Guilin 541004, China

Published online: 29 August 2018

Additionally, ion substitutions with low polarizability (P) in $CaO–B_2O_3–SiO_2$ glass–ceramic would obtain new LTCC systems with low permittivity and high quality factor. Since the dielectric properties are associated with crystallization phase precipitated in the glass. In general, the crystallization temperature of divalent metal phosphate or borate crystals precipitated from borophosphate glasses is less than 900 °C and divalent metal phosphate or borate compound has low dielectric constant and high quality factor [12, 13]. The above reports indicate that the glass–ceramic containing divalent metal borophosphate as the main crystallization phase could be a novel potential LTCC material. Thus, in this work, we prepared the $CaO–ZnO–B_2O_3–P_2O_5$ (CZBP) glass–ceramics, and investigated its sintering features and microwave dielectric properties. Moreover, the compatibility of co-firing with Ag electrode was also evaluated.

2 Experimental procedures

The starting materials, including $CaCO_3$(≥ 99.0%), ZnO (≥ 99%), H_3BO_3 (≥ 99.5%), and $NH_4H_2PO_4$(≥ 99.0%) (Guo-Yao Co. Ltd, Shanghai, China), were first mixed by wet ball milling according to the glass composition of 10.0 wt% CaO—40.0 wt% ZnO—15.0 wt% B_2O_3—35.0 wt% P_2O_5, then melted at 1250 °C for 2 h. The molten solution was quenched into deionized water to form glass slag. Then, the obtained glass frits were crushed and ball milled for 12 h in ethanol. The dried glass powders were then pressed into pellets with a diameter of 12 mm and a height of 6–7 mm, under 5 MPa pressure, and sintered at 600–780 °C for 2 h in air, with a heating rate of 5 °C/min, finally naturally cooled down to room temperature.

The thermal feature of the CZBP glasses was investigated by differential scanning calorimetry (DSC, Netzsch STA-449-F3-Jupiter, Germany) using a heating rate of 10 °C/min in air, and alumina was used as the reference material. The phase structure of glass–ceramics was performed using the X-ray diffraction analysis (XRD, Bruker D8 Advance, Germany). The microstructures of the sintered samples and the compatibility of co-firing with Ag electrodes were evaluated by field emission scanning electron microscope (FE-SEM, Quanta 600 FEG, FEI) equipped with energy dispersion spectroscopy (EDS).The bulk density of the fired samples was determined by the Archimedes method. The dielectric behaviors at a microwave frequency range of 13–14 GHz were measured with the $TE_{01\delta}$ shielded cavity method with a network analyzer (N5230C, Agilent, Palo Alto, CA) [14]. The temperature coefficient of resonant frequency (τ_f) was measured in the temperature range of 25–75 °C, and calculated using the formula $\tau_f = (f_T - f_0)/f_0(T - T_0)$, where f_T and f_0 are the resonant frequencies at the measuring temperature T and T_0 (25 °C), respectively. To check the chemical compatibility between the glass–ceramic and the silver powder, 20 wt% silver was mixed with the glass powder, and then the pressed pellet was fired at 740 °C for 2 h to achieve equilibrium.

3 Results and discussion

The DTA curve and XRD pattern of the CZBP glass powder are presented in Fig. 1. The wide dispersion diffraction peak at about 25° displays that the glass sample is structurally amorphous, i.e. non-crystallized solids, as shown in insertion diagram in Fig. 1. The DTA analysis shows that glass transition temperature (Tg) is 566 °C.

A faint exothermic peak and a sharp exothermic peak observed at temperatures of 669 °C and 796 °C are related to the various stage crystallization of the glass. Further heating make the glass melt.

XRD patterns of glass–ceramics are shown in Fig. 2. When heated at 600 °C, Only $Ca_2B_2O_5$ phase is precipitated from mother glass. At 650 °C, $CaZn_2(PO_4)_2$ phase also begins to precipitate in the glass matrix. With increasing temperature from 720 to 740 °C, $Ca_2B_2O_5$ and $CaZn_2(PO_4)_2$ as the predominate phase still exist, and the third phase $Zn_3(PO_4)_2$ appears. It is observed that the diffraction peak intensities of $Ca_2B_2O_5$, $CaZn_2(PO_4)_2$ and $Zn_3(PO_4)_2$ distinctly enhance with the increase in sintering temperature from 650 to 740 °C, indicating the crystal contents of $Ca_2B_2O_5$, $CaZn_2(PO_4)_2$ and $Zn_3(PO_4)_2$ gradually increase. High sintering temperature (780 °C) slightly weakens the diffraction peak intensities of both $CaZn_2(PO_4)_2$ and $Zn_3(PO_4)_2$ phases. Obviously, the sintering temperature has a direct effect on the type and content of precipitated crystalline phase. The variety of crystal phase components as a function of sintering temperature is listed in Table 1.

The bulk density of the glass–ceramics at different sintering temperature is shown in Fig. 3. When the sintering

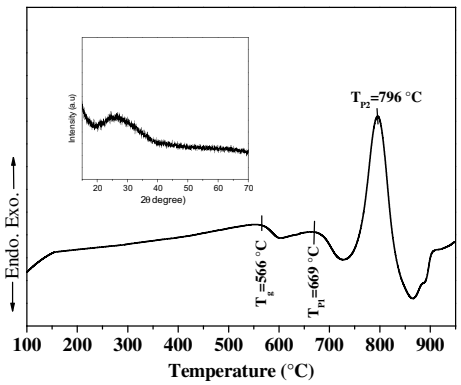

Fig. 1 DTA curve of glass powder, and insert indicates the XRD pattern of glass

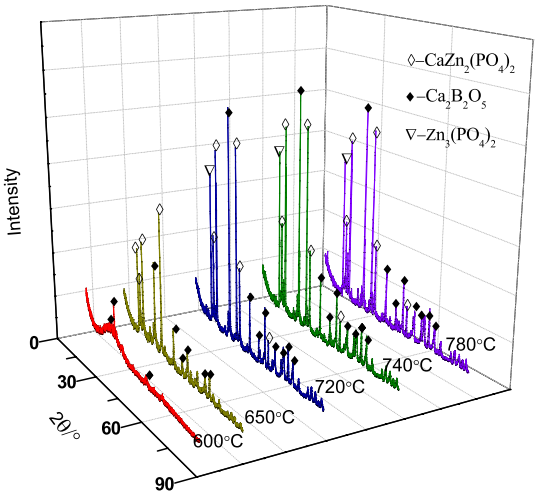

Fig. 2 XRD patterns of the glass sintered at different temperatures

temperature is 600 °C, the bulk density of the sample is 1.7663 g/cm^3. With the increase of sintering temperature, the sample is gradually densified. The maximum density of 2.9986 g/cm^3 is obtained for the sample sintered at 740 °C. However, the bulk density of the sample is slightly decreased with further increase temperature to 780 °C, which may be due to over-sintering [13].

The SEM micrographs of the glass–ceramic samples at different temperatures are presented in Fig. 4. At low temperature, i.e. 600 °C, a large number of glass phases still exist (Fig. 4a). At 650 °C, some glass powders with big size rather than precipitated crystals are observed in the sample (see Fig. 4b), and the micrographs of the sample show coexistence state of the connective open-pores, glass phase and some precipitated crystals, as shown in Fig. 4b. With increasing sintering temperature from 650 to 740 °C, it appears that open-pores in the samples gradually disappear, the contents of precipitated crystals are increased and dense microstructure is formed shown in Fig. 4c, d. At the same time, it is observed that a large number of micro-grains buried in glass phases appear in the samples (see Fig. 4c–e). However, it is noticed that the phenomenon of over-heating occurs in the sample when the sintering temperature exceeds 780 °C, as shown in Fig. 4e, which leads to the decrease in densification degree.

The variation of the dielectric constant of the glass–ceramic with the temperature is shown in Fig. 5. The dependence of ε_r of glass–ceramics on sintering temperature has a tendency similar to that of the bulk density. When heated at 600 °C, the sample has the minimum dielectric constant because of un-dense microstructure and a large amount of glass phases with lower permittivity. At 650 °C, the dielectric constant of the sample increases suddenly, which may be due to existence of the main crystalline phase $Ca_2B_2O_5$ with a large dielectric constant ($\varepsilon_r = 8.13$). When raising firing temperature from 720 to 780 °C, the dielectric constant is obviously decreased, and finally shows a little change tendency (~4.3). As well known, the dielectric properties of a material are mainly determined by the summation of each phase presented in the material. In the glass–ceramics, the ε_r of $Ca_2B_2O_5$, $CaZn_2(PO_4)_2$ and $Zn_3(PO_4)_2$ is about 8.13, 4.6 and 4.6, respectively. As mentioned above, raising temperature promotes the crystallization of $CaZn_2(PO_4)_2$ and $Zn_3(PO_4)_2$, the relative lower ε_r could be attributed to the increase of $CaZn_2(PO_4)_2$ and $Zn_3(PO_4)_2$ phases with a lower

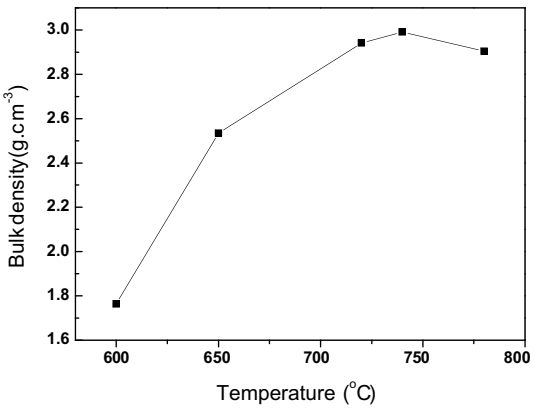

Fig. 3 Bulk density of the glass–ceramic sample as a function of sintering temperatures

Table 1 Variation of phase composition of samples at different temperatures for 4 h

Temperature/°C	Phase composition	Variation trend of phase
600	$Ca_2B_2O_5$	A small amount
650	$Ca_2B_2O_5$, $CaZn_2(PO_4)_2$	$Ca_2B_2O_5$↑
720	$Ca_2B_2O_5$, $CaZn_2(PO_4)_2$, $Zn_3(PO_4)_2$	$Ca_2B_2O_5$↑, $CaZn_2(PO_4)_2$↑↑
740	$Ca_2B_2O_5$, $CaZn_2(PO_4)_2$, $Zn_3(PO_4)_2$	$Ca_2B_2O_5$↑, $CaZn_2(PO_4)_2$↑↑, $Zn_3(PO_4)_2$↑↑
780	$Ca_2B_2O_5$, $CaZn_2(PO_4)_2$, $Zn_3(PO_4)_2$	$Ca_2B_2O_5$↓, $CaZn_2(PO_4)_2$↓, $Zn_3(PO_4)_2$↓

"↑" represents an increase in content of precipitated crystalline phase; "↓" represents an decrease in content of precipitated crystalline phase; "↑↑" represents an further increase in content of precipitated crystalline phase

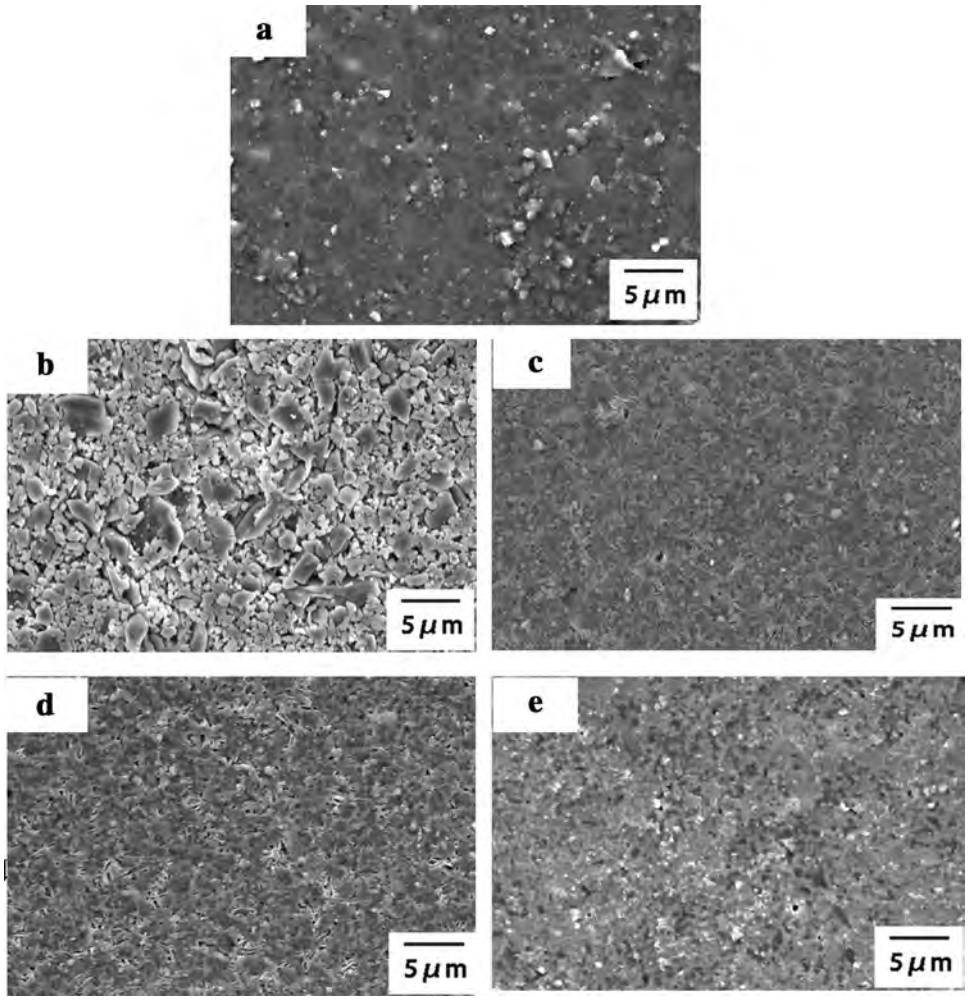

Fig. 4 SEM images of the glass–ceramic samples at different sintering temperatures. **a** 600 °C, **b** 650 °C, **c** 720 °C, **d** 740 °C, **e** 780 °C

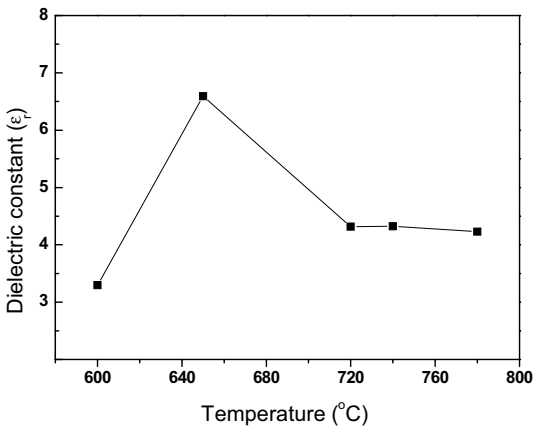

Fig. 5 Dielectric constant of glass–ceramics at various temperatures

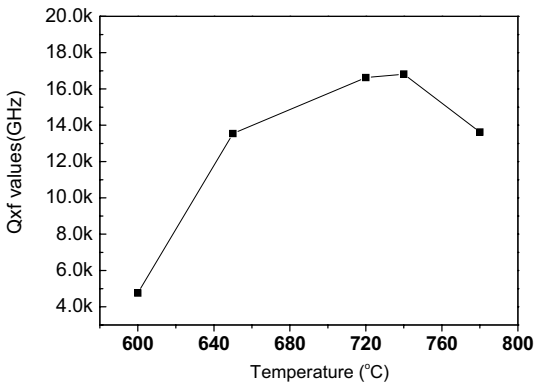

Fig. 6 Quality factor (Q×*f*) of glass–ceramics sintered at various temperatures

ε_r than that of $Ca_2B_2O_5$. However, dense microstructure has almost no impact on the dielectric constant.

Figure 6 shows Q×*f* values of glass–ceramics at different sintering temperatures. With the increase of sintering temperature, Q×*f* values exhibit first increase and then decrease, and the maximum Q×*f* value of 16,800 GHz is achieved at 740 °C. The Q×*f* value was affected not only by the intrinsic loss such as the lattice vibrational modes, but also by the pores and crystal phases [14, 15]. In this

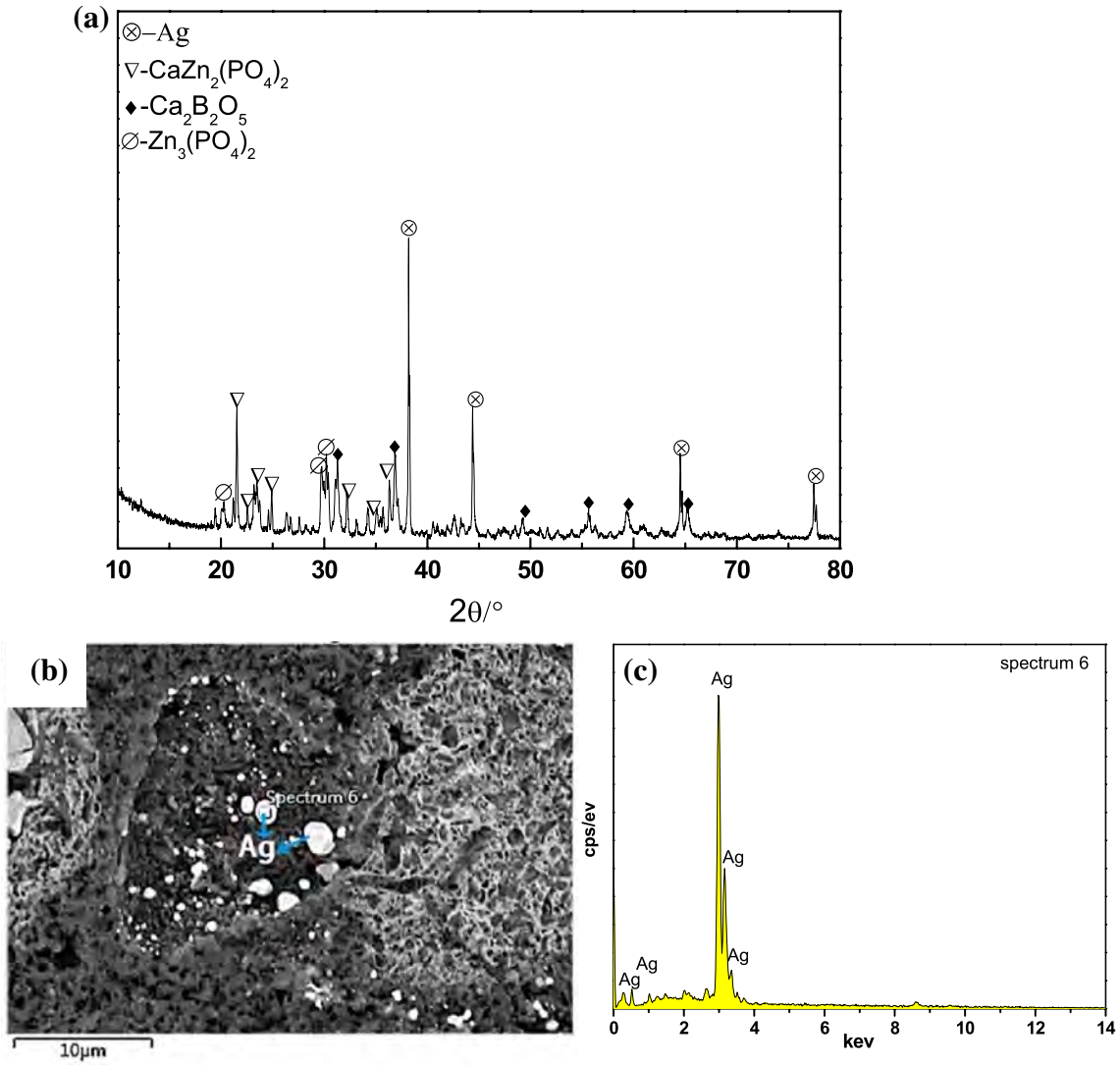

Fig. 7 XRD pattern (**a**), SEM image (**b**) and EDS analysis (**c**) of glass ceramic and silver co-fired at 740 °C for 2 h

Table 2 Processing temperatures and microwave properties of some typical glass-ceramic materials

Glass–ceramic system	Firing temperature (°C)	ε_r	Q×*f* (GHz)	τ_f (ppm/°C)
$MgO–B_2O_3–SiO_2$ [9]	850–950	6.1–6.9	5000–8000	/
$CaO–B_2O_3–SiO_2$ [10]	765–1290	4.0–7.9	~2200	/
$MgO–Al_2O_3–SiO_2–TiO_2–P_2O_5$ [16]	970	4.0	13,785	−6.4
$MgO–Al_2O_3–SiO_2–TiO_2–Sb_2O_3$ [17]	930	3.65	7900	−7.92
$CaO–B_2O_3–SiO_2$+LB [18]	850	6.26	10,040	/
$CaO–ZnO–B_2O_3–P_2O_5$ [this work]	650–780	4.2–6.5	13,450–16,826	−21.2 to −25.4

study, Q×*f* value is primarily dependent on the remnant glass phase, crystalline phase and densification of glass–ceramics. It is known that the Q×*f* value of $Ca_2B_2O_5$ and $CaZn_2(PO_4)_2$ is 8000 GHz and 18,000 GHz, respectively [9], and the Q×*f* value of $Zn_3(PO_4)_2$ measured experimentally is approximately 23,000 GHz (13.9 GHz). Increasing temperature enhances the sintering densification and crystallization. It is noted that the residual glass decreases with the increase in the total amount of crystalline phases, which means that a higher Q×*f* value will be obtained. At 600 °C, the sample

has the lowest Q×*f* value, which is due to the existence of glass phases with lower Q×*f* value. When fired at 650 °C, The amount of glass phase is decreases, and the Q×*f* value obviously increases because both $Ca_2B_2O_5$ and $CaZn_2(PO_4)_2$ have a bigger Q×*f* value than that of glass phase. With further increasing temperature from 720 to 740 °C, the monotonously increased Q×*f* values could be attributed to the relatively increasing contents of $CaZn_2(PO_4)_2$ and $Zn_3(PO_4)_2$ with higher Q×*f* value than that of $Ca_2B_2O_5$. Certainly, dense microstructure has positive influence on Q×*f* value. At 780 °C, the Q×*f* value slightly reduces, which could be ascribed to the relative content change of $Zn_3(PO_4)_2$, $CaZn_2(PO_4)_2$ and $Ca_2B_2O_5$. The decrease in the total amount of three crystalline phases results in low Q×*f* value.

The τ_f values of the samples sintered at 600 °C, 650 °C, 720 °C, 740 °C and 780 °C are − 21.2 ppm/°C, − 23.1 ppm/°C, − 21.4 ppm/°C, − 27.7 ppm/°C and − 25.4 ppm/°C, respectively. Clearly, the τ_f values are not sensitive to firing temperature.

Figure 7 depicts XRD patterns, SEM profile and EDS result of glass ceramic + 20 wt% Ag sintered at 740 °C for 2 h. From the XRD pattern, co-firing with Ag powders does not produce a new phase other than metallic silver, $Ca_2B_2O_5$, $CaZn_2(PO_4)_2$ and $Zn_3(PO_4)_2$ in the glass–ceramic sample. This observation is also confirmed by the SEM and EDS analysis (Fig. 7b, c). The SEM analysis indicates no interaction forming new phases after firing, and it is obvious that the reaction of glass–ceramic and Ag powders does almost not occur from the EDS result. Hence, this would benefit commercial applications in LTCC field.

Comparing with some typical glass–ceramic materials with low permittivity, as shown in Table 2, the as-prepared glass–ceramic possesses reasonable processing temperatures and good microwave dielectric properties.

4 Conclusions

The glass–ceramic with composition (in wt%) of 10.0 CaO–40.0ZnO–15.0 B_2O_3–35.0P_2O_5 were prepared through a solid-state reaction method. The glass–ceramic sintered at 740 °C for 2 h exhibits good microwave dielectric properties with $\varepsilon_r = 4.32$, Q×*f* = 16,800 GHz (at 13.9 GHz) and $\tau_f = -27$ ppm/°C. The merit for the glass–ceramic is its good compatibility with the Ag electrode. This finding suggests the as-obtained glass–ceramics could be a promising candidate for LTCC applications.

Acknowledgements This work was financially supported by National Undergraduate Innovation Program of the Ministry of Education of China (Nos. 201810595014, 201810595015), Undergraduate Innovation Program of Guangxi (No. 201610595186) and the Research funds of The Guangxi Key Laboratory of Information Materials (No. 171002-Z).

References

1. H.H. Xi, D. Zhou, H.D. Xie, B. He, Q.P. Wang, R. Spectra, Infrared spectra, and microwave dielectric properties of low-temperature firing $[(Li_{0.5}Ln_{0.5})_{1-x}Ca_x]MoO_4$ (Ln = Sm and Nd) solid solution ceramics with scheelite structure. J. Am. Ceram. Soc. **98**, 587–593 (2015)
2. C.C. Xia, D.H. Jiang, G.H. Chen, Y. Luo, B. Li, C.L. Yuan, C.R. Zhou, Microwave dielectric ceramic of $LiZnPO_4$ for LTCC applications. J. Mater. Sci.: Mater. Electron. **28**, 12026–12031 (2017)
3. M.S. Ma, Z.Q. Fu, Z.F. Liu, Y.X. Li, Fabrication and microwave dielectric properties of CuO-B_2O_3-Li_2O glass-ceramic with ultra-low sintering temperature. Ceram. Int. **43**, S292–S295 (2017)
4. H.F. Zhou, X.H. Tan, J. Huang, N. Wang, G.C. Fan, X.L. Chen, Phase structure, sintering behavior and adjustable microwave dielectric properties of $Mg_{1-x}Li_{2x}Ti_xO_{1+2x}$ solid solution ceramics. J. Alloys Compd. **696**, 1255–1259 (2017)
5. M.T. Sebastian, H. Wang, H. Jantunen, Low temperature co-fired ceramics with ultra-low sintering temperature: a review. Curr. Opin. Solid State Mater. **20**, 151–170 (2016)
6. S. Rajesh, H. Jantunen, Low temperature sintering and dielectric properties of alumina-filled glass composites for LTCC applications. Int. J. Appl. Ceram. Technol. **9**, 52–59 (2012)
7. D. Zhou, C.A. Randall, A. Baker, H. Wang, L.X. Pang, X. Yao, Dielectric properties of an ultra-low-temperature cofiring $BiMo_2O_9$ multilayer. J. Am. Ceram. Soc. **93**, 1443–1446 (2010)
8. H.T. Yu, K. Ju, K.M. Wang, A novel glass-ceramic with ultra-low sintering temperature for LTCC application. J. Am. Ceram. Soc. **97**, 704–707 (2014)
9. U. Došler, M.M. Kržmanc, D. Suvorov, The synthesis and microwave dielectric properties of $Mg_3B_2O_6$ and $Mg_2B_2O_5$ ceramics. J. Eur. Ceram. Soc. **30**, 413–418 (2010)
10. C.C. Chiang, S.F. Wang, Y.R. Wang, W.C.J. Wei, Densification and microwave dielectric properties of CaO–B_2O_3–SiO_2 system glass–ceramics. Ceram. Int. **34**, 599–604 (2008)
11. I.J. Induja, M.T. Sebastian, Microwave dielectric properties of SnO-SnF_2-P_2O_5 glass and its composite with alumina for ULTCC applications. J. Am. Ceram. Soc. **1**, 1–9 (2017)
12. Y.J. Chu, J.H. Jean, Low-fire processing of microwave $BaTi_4O_9$ dielectric with crystalline CuB_2O_4 and $BaCuB_2O_5$ additives. Ceram. Int. **39**, 5151–5158 (2013)
13. H. Zhu, M. Liu, H. Zhou, L. Li, A. Lv, Study on properties of CaO–B_2O_3–SiO_2 system glass–ceramic. Mater. Res. Bull. **42**, 1137–1144 (2007)
14. B.W. Hakki, P.D. Coleman, A dielectric resonator method of measuring inductive capacities in the millimeter range. IEEE Trans. Microw. Theory Techn. **8**, 402–410 (1960)
15. B.D. Silverman, Microwave Absorption in cubic strontium titanate. Phys. Rev. **125**, 1921–1930 (1962)
16. X.P. Huang, C.L. Yuan, X.Y. Liu, F. Liu, Q. Feng, J.W. Xu, C.R. Zhou, G.H. Chen, Effects of P_2O_5 on crystallization, sinterability and microwave dielectric properties of MgO-Al_2O_3-SiO_2-TiO_2 glass-ceramics. J. Non-Cryst. Solids **459**, 123–129 (2017)
17. J.J. Qu, F. Liu, C.L. Yuan, G.H. Chen, X.P. Huang, R.F. Ma, Effects of two-step heat treatment on crystallization behavior, densification and microwave dielectric properties of MgO-Al_2O_3-SiO_2-TiO_2-Sb_2O_3 glass-ceramics. J. Non-Cryst. Solids **471**, 400–405 (2017)
18. X.H. Zhou, E.Z. Li, S.L. Yang, B. Li, B. Tang, Y. Yuan, S.R. Zhang, Effects of La_2O_3-B_2O_3 on the flexural strength and microwave dielectric properties of low temperature co-fired CaO-B_2O_3-SiO_2 glass–ceramic. Ceram. Int. **38**, 5551–5555 (2012)